Journal of Solid Mechanics Vol. 10, No. 1 (2018) pp. 110-123

Nonlinear Dynamic Analysis of Cracked Micro-Beams Below and at the Onset of Dynamic Pull-In Instability

R. Hassannejad *, Sh. Amiri Jahed

Department of Mechanical Engineering, University of Tabriz, Tabriz, Iran

Received 2 November 2017; accepted 1 January 2018

ABSTRACT

In this paper, the effect of the crack on dynamic behavior of cracked micro-beam in the presence of DC and AC loads are investigated. By applying the residual axial stress and fringing field stress, a nonlinear analytical model of cracked micro-beam is presented and crack is modeled by a massless rotational spring. The governing equation of the system is solved using Galerkin procedure and shooting method. The equilibria curve and dynamic response of cracked cantilever and clamped-clamped micro-beam are extracted below and at the onset of the dynamic pull-in instability. The results show that the behavior of cracked micro-beam is different from ordinary cracked beam due to nonlinear effects. For a fixed relative crack location, increasing the crack depth causes increasing in the resonance amplitude and reduction in the resonance frequency below dynamic pull-in instability. Also, in cracked cantilever micro-beams, by approaching the crack to fixed end, the resonance frequency reduces and the resonance amplitude increases. In cracked clamped-clamped micro-beam, trend of variations of resonance frequency and resonance amplitude against the crack location is not regular. At the onset pull-in instability, the presence of the crack causes cyclic-fold bifurcation points to appear at the lower frequency. Therefore, it causes early pull-in phenomenon or unwanted abrupt change at the micro-beam behavior. The achievement of this study is simulation of the response of the faulty low-voltage switch and MEMS resonators for different severity of crack at the onset of dynamic pull-in phenomenon.

Keywords: Micro-electromechanical systems; Crack; Pull-in phenomenon; Nonlinear dynamics; Bellow and at the onset of pull-in instability.

1 INTRODUCTION

TODAY, by increasing development of technology, use of micro-electromechanical systems (MEMS) and structures increases in various techniques such as astronavigation, radars, telecommunication and biotechnology. Capacitive micro-switches and resonant micro-sensors and pressure Sensor are some of these systems. There are a number of actuation methods for MEMS devices. Electrostatic actuation is the most well-established of this actuation method because of its simplicity and high efficiency [1]. The electric load is composed of a DC polarization voltage and an AC voltage. The DC component applies an electrostatic force on the micro-beam, thereby deflecting it to a new equilibrium position, while the AC component vibrates the micro-beam around this equilibrium position [2]. The studies show that, the nonlinear behavior of micro-beams is the result of reaction

*Corresponding author. Tel.: +98 041 33393057; Fax: +98 041 33354153.
E-mail address: hassannejhad@tabrizu.ac.ir (R. Hassannejad).

of several forces such as electrostatic force and mechanical restoring force, which are considered as nonlinear terms in the governing equation. The mechanical restoring force is arising from residual, axial and fringing stress [3, 4]. When the excitation voltage increases, the balance of the forces is upset and the electric force becomes more than mechanical restoring force and it makes the micro-beam collapse and hence the failure of the device. This structural instability is known as pull-in phenomenon and the corresponding voltage is considered as pull-in voltage. This phenomenon is one of the most significant challenges in designing MEMS. The importance of the knowing the exact amount of voltage, especially in capacitive structures, is the determination of sensitivity, frequency response, dynamic rate and distortion by it. One can use the pull-in voltage to determine material characteristics such as Young modulus and residual stress [5]. Zhang and Zhao [6] studied the pull-in instability of micro-structure under electrostatic loading, using one mode analysis method. They showed that there was little difference with the established multi-mode analysis on predicting the pull-in voltage for three different structures (cantilever, clamped-clamped beams and plate with four edges simply-supported) in low axial loading range. Rezazadeh et al. [7] extracted the static pull-in voltage of two elastic parallel fixed-fixed and cantilever micro-beams in MEMS under nonlinear effects such as residual stresses, fringing field and axial stresses. They showed that, the percentage of pull-in voltage reduction when compared these micro-beams to simple fixed-fixed and cantilever models is of the order of 27-30%. Mojahedi et al. [8] investigated the pull-in instability of electrostatically actuated micro-bridges and micro-cantilevers considering different nonlinear effects. They studied the influence of mid-plane stretching, electrostatic actuation and axial loading on the static deflection. Wang et al. [9] investigated the pull-in instability and vibrational behaviors for a prestressed multi-layer micro-beam with nonlinearities arise simultaneously from electrostatic loads and large deformation. They used the same algorithm to the small amplitude free vibration around the predeformed bending configuration following an assumed harmonic time mode. The influences of pivotal parameters on the pull-in instability behavior and natural frequency were examined, including the length, thickness and residual stress of the micro-beam. Mohammad and Ouakad [10] investigated the structural behavior of a MEMS system arch micro-beam actuated by electric fringing fields where the electrodes are located at both side of the micro-beam. The results showed elimination of the pull-in instability in this kind of systems as compared to the regular case of parallel-plates electrostatic actuation. Younis [11] presented exact analytical solutions for the electrostatically actuated initially deformed cantilever micro-beam problem. They used a continuous beam model and a single-mode Galerkin technique and derived analytical expression for two commonly observed deformed beams configuring the curled and titled. Mohammadi-Alasti et al [12] studied the dynamic behavior of a functionally graded cantilever micro-beam and its pull-in instability, subjected to simultaneous effects of a thermal moment and nonlinear electrostatic pressure. According to the research results for application of a step DC voltage on thermally actuated micro-beam, when the temperature changes get higher, the pull-in voltage decreases and consequently the pull-in time increases. For a given primal temperature change, by decreasing the ceramic constituent percent, firstly the dynamic pull-in voltage due to decreasing the primal thermal deflection was increased and next due to decreasing the micro-beam stiffness, it was decreased. Also, the effect of viscous damping on the pull-in phenomenon was shown.

Most of the research investigated stability of static deflection of micro-beams. But the MEMS devices are often dynamically excited and the research shows that, there is a possibility for a dynamic instability to trigger pull-in below the statically predicted instability limit. Therefore, the analysis of the behavior of micro-beams under the AC loading is important and necessary, because of the nonlinear behavior of MEMS systems. In this regard, Nayfeh et al. [13] investigated the dynamic pull-in instability and pull-in phenomenon characteristics in the presence the combination of AC and DC and formulated safety criteria near one of their natural frequency. They also used this phenomenon to design a low-voltage MEMS RF switches actuated with a combined DC and AC loading. Rezazadeh et al. [14] studied the static and dynamic responses of a fixed–fixed and cantilever micro-beam, using both the lumped and the distributed models. They introduced design corrective coefficients. Multiplying these design coefficients with the static pull-in voltage of the lumped model, the static and dynamic pull-in voltage of a given micro-beam can be obtained without the need to solve the nonlinear governing equations. Sedighi et al. [15] investigated the effect of the amplitude of vibrations on the pull-in instability and nonlinear natural frequency of doubled-sided actuated microswitch by using nonlinear frequency amplitude. They used the Hamiltonian approach (HA). They indicated in their research that first term in series expansions is sufficient to produce acceptable accurate solutions.

There is a possibility of failure such as crack, during manufacturing and performance of MEMS. The crack increases the flexibility of micro-beam at the crack location and changes its characteristics such as mode shape, natural frequency and dynamic response. This fault causes change in the stability threshold and leads to untimely pull-in phenomenon. Micro-electromechanical structures utilize brittle material such as polycrystalline silicon (polysilicon) under potentially severe mechanical and environmental loading conditions. These structures may be

subjected to high frequency and cyclic loading conditions. The researches of the Failure analysis associates show that Silicone materials are brittle in ambient air and there is the possibility of the initiation and growth of the crack in the silicone MEMS devices [16]. Studies in the field of faulty micro-beams show that the crack leads to reduction in the pull-in voltage and the structure triggers pull-in bellow the predicted pull-in voltage of intact micro-beam. Motallebi et al. [17] investigated the effect of the open crack depth ratio, crack position and crack number on the pull-in voltage in the cracked micro-beam with clamped-clamped and cantilever boundary condition bellow the pull-in instability. In their work the dynamic pull-in voltage is defined as a step DC voltage, which is applied suddenly and leads to instability of system. They solved the governing equation by step by step linearization method (SSLM) and Galerkin-based reduced order model. Zhou et al. [18] investigated the effect of slant open crack on the mode shape, natural frequency and pull-in voltage of fixed-fixed micro-beam in different crack depths, location and slant angle bellow the pull-in instability. They showed the crack position has more significant influence on the pull-in voltage value than the slant angle or the depth ratio. They extracted the dynamic response of fixed-fixed micro-beam in the area far from pull-in phenomenon using single mode and perturbation method. Sourki et al [19] investigates the analysis for free transverse vibration of a cracked micro-beam based on the modified couple stress theory within the framework of Euler–Bernoulli beam theory. In this investigation, the influence of diverse crack position, crack severity, material length scale parameter as well as various Poisson's ratio on natural frequencies was studied. The results illustrate that the aforementioned parameters are playing a significant role on the dynamic behavior of the micro-beam.

Existing research in literature shows that, there are few studies on the effects of cracks on the micro-beams. In these researches, the dynamic behavior of cracked micro-beam under AC voltage was not investigated at the onset of dynamic pull-in phenomenon. Also the effect of crack on the dynamic behavior (resonance amplitude and resonance frequency) of cracked micro-beam with cantilever boundary condition was not studied. Therefore, in this paper the effect depth and location of the crack is investigated on the static and dynamic pull-in instability bellow and at the onset of dynamic pull-in instability. The dynamic behavior of cracked micro-sensors and micro-switches are simulated as a continuous model of cracked micro-beam with the boundary condition of clamped-clamped and cantilever. In this model nonlinear electrical and mechanical force such as fringing field and residual axial force are considered. The crack was modeled as massless rotational spring and its stiffness is extracted using principles of fracture mechanics. The governing equation of cracked micro-beam is discretized onto a finite-degree-of-freedom system consisting of ordinary-differential equations, by means of reduced-order-model. Furthermore, using combination of two point-boundary-value problem and shooting method, the governing equation is solved and the response is extracted. The static and dynamic response of cracked micro-sensors and micro-switches are extracted near natural frequency bellow and at the onset of dynamic pull-in instability for different crack depth and crack location. The effect of the fringing field force is neglect in the extracting of the curves of static and dynamic behavior of cracked micro-beam; because its value is less than 2 % of excitation force.

2 MATHEMATICAL MODELING OF CRACKED MICRO-BEAM

A schematic of view of single-edge cracked cantilever and clamped-clamped micro-beam, subjected to viscous damping with a coefficient $\hat{c}$ per unit length and actuated by electric load, $F=\frac{1}{2}\varepsilon b\frac{\left[V(\hat{t})\right]^2}{\left(d-\hat{w}\right)^2}(1+F_r)$, is illustrated in Fig. 1. The electric load is composed of a DC polarization voltage and an AC voltage. The dynamic behavior of the cracked micro-beam is modeled as Euler-Bernoulli beam of length L, width b, thickness h, which the crack divides it into two segments. The governing equations of the transverse vibration of two segments of micro-beam are [20, 21]:

$$EI\frac{\partial^4\hat{w}_1}{\partial\hat{x}^4}+\rho bh\frac{\partial^2\hat{w}_1}{\partial t^2}+\hat{c}\frac{\partial\hat{w}_1}{\partial t}=\left[\hat{N}_a+\hat{N}_r\right]\frac{\partial^2\hat{w}_1}{\partial\hat{x}^2}+\frac{1}{2}\varepsilon b\frac{\left[V(\hat{t})\right]^2}{\left(d-\hat{w}_1\right)^2}(1+F_{r1}),\qquad 0\le\hat{x}\le L_o \tag{1}$$

$$EI\frac{\partial^4\hat{w}_2}{\partial\hat{x}^4}+\rho bh\frac{\partial^2\hat{w}_2}{\partial t^2}+\hat{c}\frac{\partial\hat{w}_2}{\partial t}=\left[\hat{N}_a+\hat{N}_r\right]\frac{\partial^2\hat{w}_2}{\partial\hat{x}^2}+\frac{1}{2}\varepsilon b\frac{\left[V(\hat{t})\right]^2}{\left(d-\hat{w}_2\right)^2}(1+F_{r2}),\qquad L_o\le\hat{x}\le L \tag{2}$$

where $\hat{x}$ is the position along the micro-beam, A and I are the area and moment of inertia of the cross-section, E is Young modulus, $\hat{N}_r$ is the residual axial force, ρ is the material density, d is the capacitor gap width and ε is the dielectric constant of gap medium. L_0 is the distance of crack from fixed end. The $N_a = \frac{EA}{2L}\left(\int_0^{L_0}\left(\frac{\partial \hat{w}_1}{\partial \hat{x}}\right)^2 d\hat{x} + \int_{L_0}^{L}\left(\frac{\partial \hat{w}_2}{\partial \hat{x}}\right)^2 d\hat{x}\right)$ is the tensile axial force, which for the case of cantilever micro-beam is not account and the first order fringing field correction is denoted as $F_{ri} = 0.65\frac{(d-\hat{w}_i)}{b}$, $i = 1,2$ [5]. Eqs. (3) and (4) are the boundary conditions of clamped-clamped and cantilever micro-beam, respectively:

$$\hat{w}_1(0,\hat{t}) = \frac{\partial \hat{w}_1(0,\hat{t})}{\partial \hat{x}} = 0, \qquad \hat{w}_2(L,\hat{t}) = \frac{\partial \hat{w}_2(L,\hat{t})}{\partial \hat{x}} = 0 \tag{3}$$

$$\hat{w}_1(0,\hat{t}) = \frac{\partial \hat{w}_1(0,\hat{t})}{\partial \hat{x}} = 0, \qquad \frac{\partial^3 \hat{w}_2(L,\hat{t})}{\partial \hat{x}^3} - \hat{N}_r \frac{\partial \hat{w}_2(L,\hat{t})}{\partial \hat{x}} = \frac{\partial^2 \hat{w}_2(L,\hat{t})}{\partial \hat{x}^2} = 0 \tag{4}$$

In the presence of the crack, the elastic strain energy and stiffness of micro-beams reduce at the crack location. This local stiffness is modeled by placing a massless torsional spring in the location of crack (see Fig. 2). The stiffness of the spring can be calculated from the fracture mechanic [22]. To satisfy the compatibility requirements, one may equate the displacements and bending moments and shear forces of the two segments of beam at the crack location. The moment at the crack location is equals to the moment of the torsional spring. Therefore, the compatibility requirements at the crack locations are assumed as follow:

$$\begin{aligned}
&\hat{w}_1(L_0,\hat{t}) = \hat{w}_2(L_0,\hat{t}), \qquad \frac{\partial^2 \hat{w}_1(L_0,\hat{t})}{\partial \hat{x}^2} = \frac{\partial^2 \hat{w}_2(L_0,\hat{t})}{\partial \hat{x}^2},\\
&\frac{\partial^3 \hat{w}_1(L_0,\hat{t})}{\partial \hat{x}^3} - \hat{N}_r \frac{\partial \hat{w}_1(L_0,\hat{t})}{\partial \hat{x}} = \frac{\partial^3 \hat{w}_2(L_0,\hat{t})}{\partial \hat{x}^3} - \hat{N}_r \frac{\partial \hat{w}_2(L_0,\hat{t})}{\partial \hat{x}},\\
&EI\frac{\partial^2 \hat{w}_2(L_0,\hat{t})}{\partial \hat{x}^2} = \hat{K}\left(\frac{\partial \hat{w}_2(L_0,\hat{t})}{\partial \hat{x}} - \frac{\partial \hat{w}_1(L_0,\hat{t})}{\partial \hat{x}}\right)
\end{aligned} \tag{5}$$

where $\hat{K}$ is the equivalent linear stiffness of torsional spring at the crack location as a function of the crack severity. In order to facilitate the analysis and identify the vibrational characteristics of system, the following non-dimensional variables are introduced:

$$w_1 = \frac{\hat{w}_1}{d}, \qquad w_2 = \frac{\hat{w}_2}{d}, \qquad x = \frac{\hat{x}}{L}, \qquad t = \hat{t}\sqrt{\frac{EI}{\rho bhL^4}}, \qquad \Omega = \hat{\Omega}\sqrt{\frac{\rho bhL^4}{EI}} \tag{6}$$

Substituting Eq. (6) into Eq. (1) and Eq. (2), it yields:

$$\frac{\partial^4 w_1}{\partial x^4} + \frac{\partial^2 w_1}{\partial t^2} + c\frac{\partial w_1}{\partial t} = [N_a + N_r]\frac{\partial^2 w_1}{\partial x^2} + \alpha_2 \frac{(V_{DC} + V_{DC}\cos(\Omega t))^2}{(1-w_1)^2} + \alpha_3 \frac{(V_{DC} + V_{DC}\cos(\Omega t))^2}{(1-w_1)}, \qquad 0 \le x \le \beta \tag{7}$$

$$\frac{\partial^4 w_2}{\partial x^4} + \frac{\partial^2 w_2}{\partial t^2} + c\frac{\partial w_2}{\partial t} = [N_a + N_r]\frac{\partial^2 w_2}{\partial x^2} + \alpha_2 \frac{(V_{DC} + V_{DC}\cos(\Omega t))^2}{(1-w_2)^2} + \alpha_3 \frac{(V_{DC} + V_{DC}\cos(\Omega t))^2}{(1-w_1)}, \qquad \beta \le x \le 1 \tag{8}$$

where $\beta = L_0/L$ is relative distance of the beam from the fixed end. Eqs. (9) and (10) are the non-dimensional boundary conditions of clamped-clamped and cantilever micro-beams, respectively:

$$w_1(0,t)=\frac{\partial w_1(0,t)}{\partial x}=0, \qquad w_2(1,t)=\frac{\partial w_2(1,t)}{\partial x}=0 \tag{9}$$

$$w_1(0,t)=\frac{\partial w_1(0,t)}{\partial x}=0, \qquad \frac{\partial^3 w_2(1,t)}{\partial x^3}-N_r\frac{\partial w_2(1,t)}{\partial x}=\frac{\partial^2 w_2(1,t)}{\partial x^2}=0 \tag{10}$$

The non-dimensional compatibility requirements:

$$\begin{aligned} &w_1(\beta,t)=w_2(\beta,t), \qquad \frac{\partial^2 w_1(\beta,t)}{\partial x^2}=\frac{\partial^2 w_2(\beta,t)}{\partial x^2},\\ &\frac{\partial^3 w_1(\beta,t)}{\partial x^3}-N_r\frac{\partial w_1(\beta,t)}{\partial x}=\frac{\partial^3 w_2(\beta,t)}{\partial x^3}-N_r\frac{\partial w_2(\beta,t)}{\partial x},\\ &\frac{\partial^2 w_2(\beta,t)}{\partial x^2}=K\left(\frac{\partial w_2(\beta,t)}{\partial x}-\frac{\partial w_1(\beta,t)}{\partial x}\right) \end{aligned} \tag{11}$$

The parameters appearing in Eq. (7) and Eq. (8) are:

$$\begin{aligned} &c=\frac{\hat{c}l^4}{EIT}, \quad N_a=\frac{\hat{N}_a l^2}{EI}, \quad N_r=\frac{\hat{N}_r l^2}{EI}, \quad \alpha_2=\frac{6\varepsilon l^4}{Eh^3d^3}, \quad \alpha_3=\frac{3.9\varepsilon l^4}{Ebh^3d^2}, \quad \beta=\frac{L_0}{L},\\ &K=\frac{\hat{K}L}{EI}, \quad T=\sqrt{\frac{\rho bhL^4}{EI}} \end{aligned} \tag{12}$$

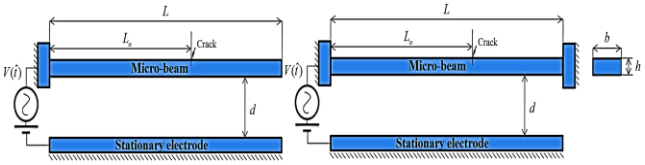

Fig.1
A schematic view of electrically actuated cracked cantilever and clamped-clamped micro-beam.

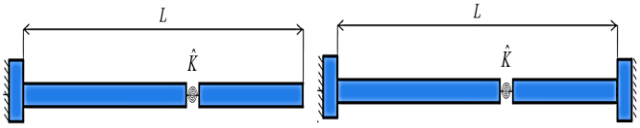

Fig.2
A graphical modeling of crack in cracked cantilever and clamped-clamped micro-beam.

3 THE REDUCED ORDER MODEL

Equation systems (7) to (11) are the nonlinear continuous system. By discretizing equations onto a finite-degree-of-freedom system consisting of ordinary-differential equations in time, a reduced-order model is generated. Assuming that the first mode is dominant mode, one can use the first undamped linear mode shapes of the micro-beam at the two side of crack, which satisfies the boundary conditions and compatibility requirement. Then the deflections of micro-beam at the two sides of the crack are:

$$w_1(x,t)=u_1(t)\phi_{11}(x), \qquad w_2(x,t)=u_1(t)\phi_{21}(x) \tag{13}$$

where, $u_1(t)$ is the first generalized coordinate, $\phi_{11}(x)$ and $\phi_{21}(x)$ are the first undamped linear mode shapes of the micro-beam at the two sides of the crack, normalized such that $\int_0^\beta \phi_{11}^2 dx+\int_\beta^1 \phi_{21}^2 dx=1$ and governed by:

$$\phi_{11}^{iv} = N\phi_{11}'' + \omega_1^2\phi_{11} \tag{14}$$

$$\phi_{21}^{iv} = N\phi_{21}'' + \omega_1^2\phi_{21} \tag{15}$$

$$\phi_{11}(0)=0, \qquad \phi_{11}'(0)=0, \qquad \phi_{21}(1)=0, \qquad \phi_{21}'(1)=0 \tag{16}$$

$$\phi_{11}(0)=0, \qquad \phi_{11}'(0)=0, \qquad \phi_{21}''(1)=0, \qquad \phi_{21}(1)-N_r\phi_{21}'(1)=0 \tag{17}$$

$$\begin{aligned}&\phi_{11}(\beta)=\phi_{21}(\beta), \qquad \phi_{11}'''(\beta)-N_r\phi_{11}'(\beta)=\phi_{21}'''(\beta)-N_r\phi_{21}'(\beta), \qquad \phi_{11}''(\beta)=\phi_{21}''(\beta),\\ &\phi_{21}''(\beta)=K(\phi_{21}'(\beta)-\phi_{11}'(\beta))\end{aligned} \tag{18}$$

Here, ω_1 is the first natural frequency of the cracked micro-beam. Eqs. (16) and (17) are related to boundary conditions of clamped-clamped and cantilever micro-beam, respectively and the Eq.(18) is related to the compatibility requirements at the crack location. The non-dimensional spring stiffness K can be calculated from the following formula [22]:

$$K=\frac{L}{6\pi n^2 f(n)}, \qquad f(n)=0.6384-1.035n+3.7201n^2-5.1773n^3+7.553n^4-7.332n^5+2.4909n^6 \tag{19}$$

where $n=a/h$ is the relative depth of the crack. One could multiply Eq. (7) by $\phi_{11}(x)(1-w_1)^2$ and Eq. (8) by $\phi_{21}(x)(1-w_2)^2$, substitute Eq. (13) into the resulting equations and use Eq. (14) and Eq. (15) to eliminate ϕ_{j1}^{iv}, $j=1,2$. Then the outcome of first equation is integrated from $x=0$ to $x=\beta$ and the outcome of second equation is integrated from $x=\beta$ to $x=1$. Summing two equations of systems yields:

$$\begin{aligned}&\ddot{u}_1-2\ddot{u}_1u_1\left[\int_0^\beta\phi_{11}^3dx+\int_\beta^1\phi_{12}^3dx\right]+\ddot{u}_1u_1^2\left[\int_0^\beta\phi_{11}^4dx+\int_\beta^1\phi_{12}^4dx\right]+c\dot{u}_1+(\omega_1^2+\alpha_3V^2(t))u_1=(\alpha_2+\alpha_3)V^2(t)\left[\int_0^\beta\phi_{11}dx+\int_\beta^1\phi_{12}dx\right]+\\ &2u_1^2\omega_1^2\left[\int_0^\beta\phi_{11}^3dx+\int_\beta^1\phi_{12}^3dx\right]-u_1^3\omega_1^2\left[\int_0^\beta\phi_{11}^4dx+\int_\beta^1\phi_{12}^4dx\right]+2c\dot{u}_1u_1\left[\int_0^\beta\phi_{11}^3dx+\int_\beta^1\phi_{12}^3dx\right]-c\dot{u}_1u_1^2\left[\int_0^\beta\phi_{11}^4dx+\int_\beta^1\phi_{12}^4dx\right]+\\ &N_au_1^3\left[\int_0^\beta\phi_{11}\phi_{11}''dx+\int_\beta^1\phi_{12}\phi_{12}''dx\right]-2N_au_1^4\left[\int_0^\beta\phi_{11}^2\phi_{11}''dx+\int_\beta^1\phi_{12}^2\phi_{12}''dx\right]+N_au_1^5\left[\int_0^\beta\phi_{11}^3\phi_{11}''dx+\int_\beta^1\phi_{12}^3\phi_{12}''dx\right]\end{aligned} \tag{20}$$

Eq. (20) is the periodic function of time and describes the dynamic behavior of an electrically actuated cracked micro-beam. Using mathematical manipulation, one could extract an explicit equation in $\ddot{u}_1$ and solves it numerically.

4 THE EFFECT OF CRACK ON THE STATIC BEHAVIOR AND EQUILIBRIA CURVE OF CRACKED MICRO-BEAM

To simulate the static behavior of cracked cantilever and clamped-clamped micro-beam, all time-varying terms, including inertia, damping and variable forcing in Eq. (20) are set equal to zero and time-varying modal variables are replaced with constant coefficients [23]. This method results in a nonlinear algebraic equation. The calculated mode shapes are plugged into this algebraic equation and it is solved numerically and then the micro-beam static deflection is calculated. By means of this method, for the cracked cantilever micro-beam with properties cited in Table 1., the variations of maximum deflection at the free end with DC voltage was extracted for a given relative crack depth $n=0.5$ and different crack locations (see Fig. 3). According to the definition of the fringing field force and the ratio of fraction $\frac{0.65d}{b}=0.015$, the effect of this force is neglected. The value of non-dimensional residual axial force is $N_r=4$. In Fig.3, there is a saddle-node bifurcation point in the each curve. The voltage of each of

these saddle-node bifurcation points is the static pull-in voltage for various crack location. If the applied DC excitation voltage is equal or more than the static pull-in voltage the micro-beam collapses. According to this figure, approaching the crack to fixed end reduces the static pull-in voltage and Stable voltage ranges in equilibrium curve. It also decreases the difference between the points of upper branch and lower branch of each curve at a certain voltage. Moreover, approaching the crack to free end decreases the rate of static pull-in voltage drop; So that, the static pull-in voltages are very near together for crack locations around the free end of micro-beam.

Table 1
The value of variables in cantilever micro-beam.

Design variable	$L(\mu m)$	$b(\mu m)$	$h(\mu m)$	$d(\mu m)$	$\rho(kg/m^3)$	$E(Gpa)$	ν	$\varepsilon(PF/m)$
Value	250	50	3	1.18	2331	169	0.06	8.85

Fig. 4 shows the variation of maximum free end deflection of cracked cantilever micro-beam with DC voltage for a fixed relative crack location $\beta = 0.05$ and different crack depths. The results show that, by increasing depth of the crack, the static pull-in voltage and stable voltage range in equilibria curve are reduced. Also, an increase in the crack depth results in an increase in the drop rate of static pull-in voltage.

To investigate the effect of the crack on the cracked clamped-clamped micro-beam, a micro-beam with the properties listed in Table 2., and under non-dimensional residual axial force $N_r = 8.7$ is considered. Similarly in the cracked clamped-clamped micro-beam, the ratio of fraction is $\frac{0.65d}{b} = 0.007$, and then the effect of fringing field force is neglected. If the equilibria of cracked clamped-clamped micro-beam under DC loading is plotted for a given relative crack depth $n = 0.5$ and different crack locations, it can be seen that the static pull-in voltage drop is not a regular trend against crack location (See Fig. 5). The static pull-in voltage is the lowest at the crack location $\beta = 0$, 1 . By changing the location of the crack from the fixed end to relative location $\beta = 0.25,$ the value of the static pull-in voltage increases. Then this value is reduced from the relative location $\beta = 0.25,$ to middle of the micro-beam. This procedure similarly repeats from $\beta = 1$ to middle of the micro-beam, because of the geometric symmetry. Also, the equilibria of cracked clamped-clamped micro-beam under DC loading for fixed relative crack location $\beta = 0.5$ and different crack depths are shown in Fig. 6. In this figure, the reduction of static pull-in voltage of cracked clamped-clamped micro-beam against increasing of crack depth is regular trend. Also, the static pull-in voltage and stable voltage range in the equilibria curve of cracked micro-beam are so closed together for different crack depths.

One could note from Figs. 3 to 6 that crack has low effect on static pull-in and static equilibria curve. The study of these figures shows that the effect of crack on the cantilever micro-beam is more than micro-beam with clamped-clamped boundary condition. Also, in both boundary conditions, the location of the crack has more effect on static pull-in than crack depth.

Table 2
The value of variables in clamped-clamped micro-beam.

Design variable	$L(\mu m)$	$b(\mu m)$	$h(\mu m)$	$d(\mu m)$	$\rho(kg/m^3)$	$E(Gpa)$	ν	$\varepsilon(PF/m)$
Value	510	100	1.5	1.18	2331	169	0.06	8.85

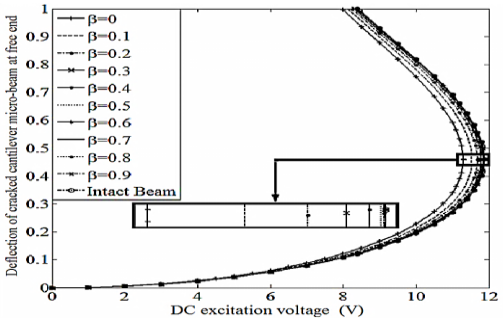

Fig.3
Equilibria of cracked cantilever micro-beam for fixed relative crack depth $n = 0.5$ and different crack locations.

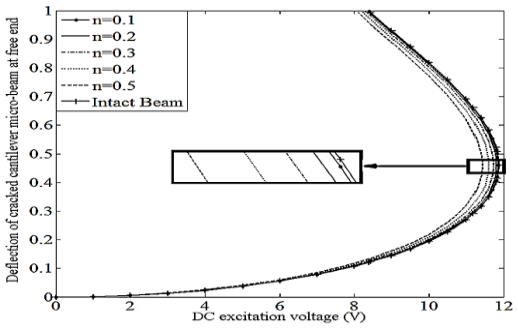

Fig.4
Equilibria of cracked cantilever micro-beam for fixed relative crack location $\beta = 0.05$ and different crack depths.

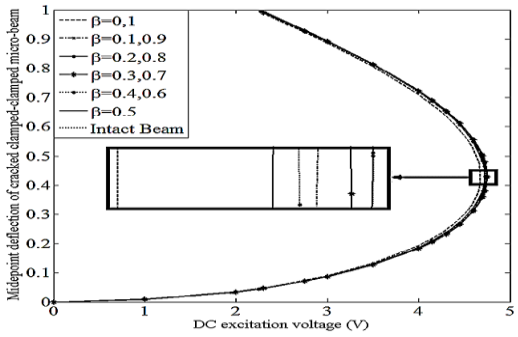

Fig.5
Equilibria of cracked clamped-clamped micro-beam for a fixed relative crack depth $n = 0.5$ and different crack locations.

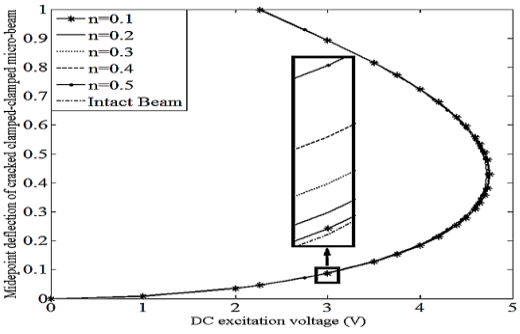

Fig.6
Equilibria of cracked clamped-clamped micro-beam for a given relative crack location $\beta = 0.5$ and different crack depths.

5 THE EFFECT OF THE CRACK ON THE DYNAMIC BEHAVIOR OF CRACKED MICRO-BEAM

The dynamic behavior of cracked cantilever micro-beam, with properties cited in Table 1., is investigated under $V_{DC} = 5\,\mathrm{V}$ and AC harmonic excitation, near its fundamental natural frequency. The non-dimensional damping coefficient is considered as $c = \omega_1 / Q$, which the quality factor is assumed as $Q = 500$. By solving Eq. (20), constitutes second-order nonlinear periodic equation, the dynamic response of cracked micro-beam is extracted.

It is used the combination a two-point boundary-value problem and shooting method to calculate periodic solution of Eq. (20). The shooting method is used for capturing periodic motion and analyzing their stability for nonlinear systems. For example, by solving Eq. (20), the frequency response of free end of cracked cantilever micro-beam can be extracted under $V_{AC} = 0.05\,\mathrm{V}$ for a fixed relative crack depth $n = 0.5$ and different crack locations (see Fig. 7). As can be seen in Fig. 7, there is no indication of pull-in phenomenon and the behavior of cracked micro-beam is softening. As the crack location gets closer to fixed end, the value of resonance frequency decreases and the resonance amplitude increases. The value of resonance frequency in intact micro-beam is $\Omega = 5.23$ and in cracked micro-beam with a crack at fixed end is $\Omega = 4.94$. By approaching the location of crack to free end, sensitivity of FRF of cracked micro-beam to crack location decreases and the frequency response curves are closed to frequency response curve of intact micro-beam. Also, the frequency response of free end of cracked cantilever micro-beam

under $V_{AC}=0.05\,\mathrm{V}$ for a fixed relative crack location $\beta=0.05$ and different crack depths is plotted in Fig. 8. Increasing the crack depth decreases the resonance frequency and increases the resonance amplitude. By increasing crack depth, the rate of changing of resonance frequency, amplitude and softening phenomenon increase.

For dynamic analysis of cracked micro-beam with clamped-clamped boundary condition, it is used the micro-beam with properties cited in Table 2. This cracked micro-beam is exited under $V_{DC}=2\mathrm{V}$ and AC harmonic voltage, near its fundamental natural frequency. The non-dimensional damping coefficient is considered as $c=\omega_1/Q$ with quality factor assuming as $Q=1000$. Fig. 9 shows the frequency response of the midpoint of cracked clamped-clamped micro-beam under $V_{AC}=0.01\mathrm{V}$ for a fixed relative crack depth $n=0.5$ and different crack locations. As can be seen in this figure, there is no indication of pull-in and the dynamic behavior of cracked micro-beam is hardening. The trend of resonance frequency and resonance amplitude changes versus crack location are not regular. The changes of resonance frequency are similar to the changes of static pull-in in Fig.5. Hence, the lowest resonance frequency is related to crack which is located near the fixed end and the highest frequency is related to location of $\beta=0.25,0.75$. Also, the changes of resonance amplitude are reverse of the changes of static pull-in voltage in Fig. 5. As shown in Fig. 9, by approaching the crack to fixed end, the rate of the changes of frequency and amplitude will have greater intensity. The frequency response of the midpoint of cracked clamped-clamped micro-beam under $V_{AC}=0.01\mathrm{V}$ for a fixed relative crack location $\beta=0.5$ and different crack depths is illustrated in Fig. 10. It follows from this figure that the resonance frequency decreases and resonance amplitude increases by increasing the crack depth.

It can be concluded from the review of Figs. 7 to 10, the presence of the crack with different depths and locations causes the changes in dynamic behavior such as resonance frequency reduction and resonance amplitude increasing near the natural frequency. These changes indicate the existence of crack in the structure and the location and intense of the crack eclipse the dynamic behavior of cracked micro-beam.

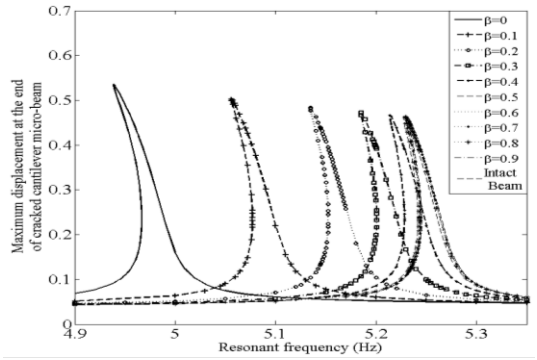

Fig.7
Frequency-response curves of cracked cantilever micro-beam for a fixed relative crack depth $n=0.5$ and different crack locations bellow the pull-in instability: $V_{DC}=5\,\mathrm{V}, V_{AC}=0.05\,\mathrm{V}$.

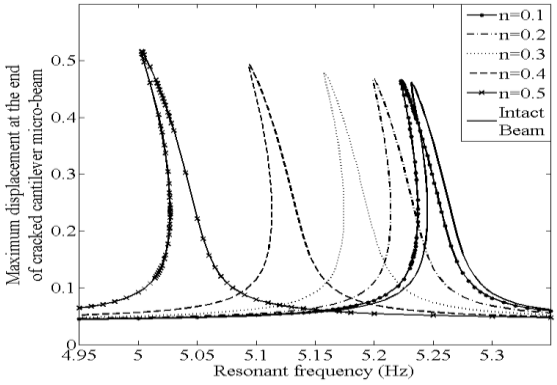

Fig.8
Frequency-response curves of cracked cantilever micro-beam for a fixed relative crack location $\beta=0.05$ and different crack depths bellow the pull-in instability: $V_{DC}=5\,\mathrm{V}, V_{AC}=0.05\,\mathrm{V}$.

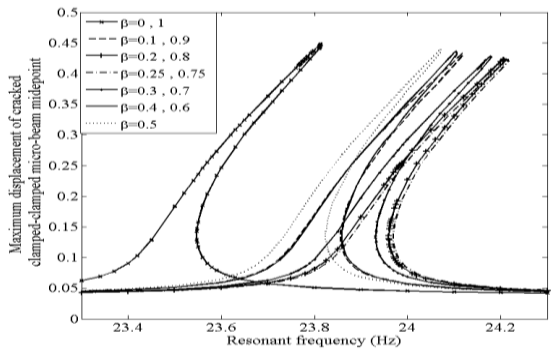

Fig.9
Frequency-response curves of cracked clamped-clamped micro-beam for a fixed relative crack depth $n = 0.5$ and different crack locations bellow the pull-in instability: $V_{DC} = 2\ \mathrm{V}, V_{AC} = 0.01\mathrm{V}$.

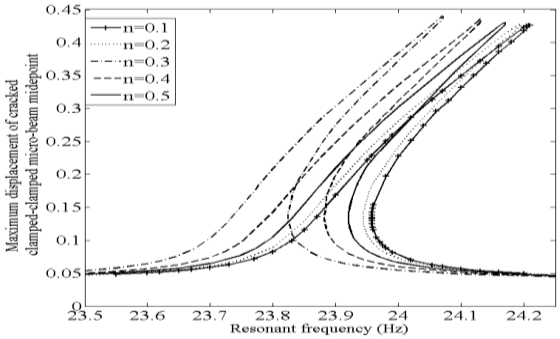

Fig.10
Frequency-response curves of midpoint of cracked clamped-clamped micro-beam for a fixed relative crack location $\beta = 0.5$ and different crack depths bellow the pull-in instability: $V_{DC} = 2\ \mathrm{V}, V_{AC} = 0.01\mathrm{V}$.

By increasing excitation voltage up to $V_{DC} = 0.1\mathrm{V}$, the dynamic pull-in phenomenon occurrence is possible in cantilever micro-beam. Fig. 11 shows the frequency response of the free end of intact cantilever micro-beam under $V_{AC} = 0.1\mathrm{V}$. The upper branches have been truncated at $W_{\max} = 0.9$ because the accuracy of the prediction of unstable branch beyond $W_{\max} = 0.9$ is dubious. The solid line denotes stable branches and the dashed line denotes an unstable branch. The stable branch collides with unstable branch at point A. The slope of curve approaches infinity in this point. As seen in Fig. 11, an up-sweep past point A will result in a jump up (to the upper stable branch) or in pull-in.

In order to investigate the effect of the crack on the behavior of cracked micro-beam at the onset of pull-in phenomenon, the frequency response of the free end of cracked cantilever micro-beam under $V_{AC} = 0.01\mathrm{V}$ for a fixed relative crack depth $n = 0.5$ and different crack locations is shown in Fig. 12. As shown in figure, by approaching crack to the fixed end, the resonance frequency is reduced and pull-in phenomenon is possible to occur at lower frequency. By reducing the distance of the crack from fixed end, the rate of reduction of resonance frequency is increased. Also, the frequency response of the free end of cracked cantilever micro-beam under $V_{AC} = 0.1\mathrm{V}$ for a fixed relative crack location $\beta = 0.05$ and different crack depths is plotted in Fig. 13. The figure shows that, increasing crack depth cause the resonance frequency to decrease and instability to occur sooner.

Similarly, by increasing excitation voltage up to $V_{DC} = 0.1\mathrm{V}$, the dynamic pull-in phenomenon in clamped-clamped micro-beam becomes possible and the shape of the curve substantially changes. Fig. 14 shows the frequency response of the midpoint of intact clamped-clamped micro-beam under $V_{AC} = 0.1\mathrm{V}$. In this case, the frequency response curve does not close within the figure. Nayfeh and et al. [13] plotted the curve of intact clamped-clamped micro-beam similar to Fig. 14, using three modes in Galerkin procedure. In Fig. 14 the dotted-dashed line represents a branch of saddles. There are three cyclic-fold bifurcations where a stable branch collides with unstable branch of solutions. The slope of curve approaches infinity in these points. As seen in this figure, an up-sweep past point A will result in a jump up (to upper stable branch) or down (to the lower right stable branch) or in pull-in. A down-sweep past point B will result in a jump up (to left stable branch or upper stable branch) or in pull-in. An up-sweep past point C will results in a jump down (to the lower right stable branch) or in pull-in. These points are undesirable points, because the behavior of the micro-beam changes suddenly in these points and the pull-in phenomenon is possible.

In order to investigate the effect of the crack on the behavior of cracked micro-switch at the onset of pull-in phenomenon, the frequency response of the midpoint of cracked clamped-clamped micro-beam under $V_{AC} = 0.1\mathrm{V}$

for a fixed relative crack depth $n = 0.5$ and different crack location is shown in Fig. 15. In this the figure, changes of resonance frequency and resonance amplitude near the natural frequency against the changes of crack depth is similar to Fig. 9. As can be seen in Fig. 15, the effect of the crack on the cyclic-fold bifurcation *A, B* and *C* is more than the other points of figure and the curves of various crack location are completely separated in these points. Also, these curves are close together in the points far from the resonance frequency and the crack has low effect on the curves in these points.

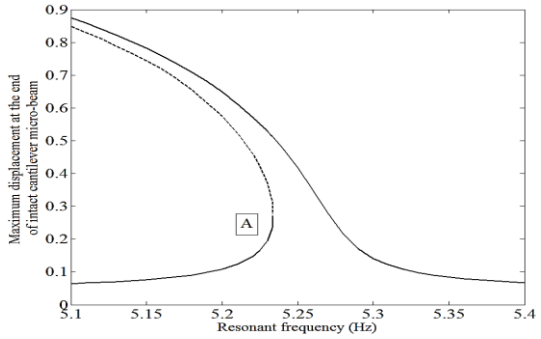

Fig.11
Frequency-response curve of free end of intact cantilever micro-beam at the onset of the pull-in instability: $V_{DC} = 5\ \text{V}, V_{AC} = 0.1\text{V}$.

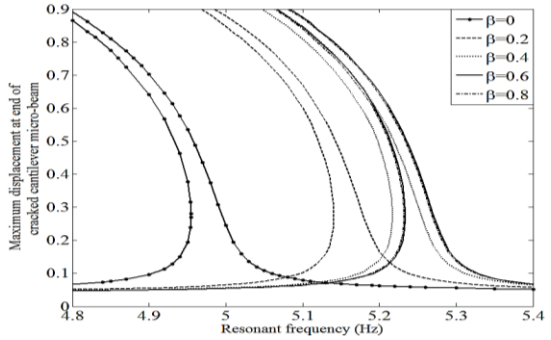

Fig.12
Frequency-response curves of free end of cracked cantilever micro-beam for a fixed relative crack depth $n = 0.5$ and different crack locations at the onset of the pull-in instability: $V_{DC} = 5\ \text{V}, V_{AC} = 0.1\text{V}$.

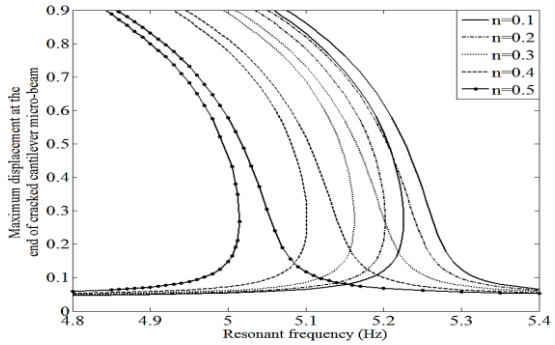

Fig.13
Frequency-response curves of free end of cracked cantilever micro-beam for a fixed relative crack location $\beta = 0.05$ and different crack depths at the onset of the pull-in instability: $V_{DC} = 5\ \text{V}, V_{AC} = 0.1\text{V}$.

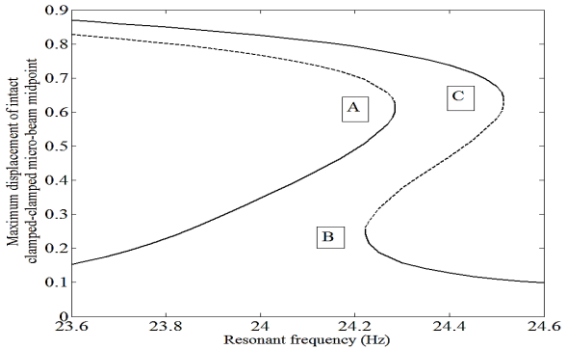

Fig.14
Frequency-response curve of midpoint of intact clamped-clamped micro-beam at the onset of the pull-in instability: $V_{DC} = 2\ \text{V}, V_{AC} = 0.1\text{V}$.

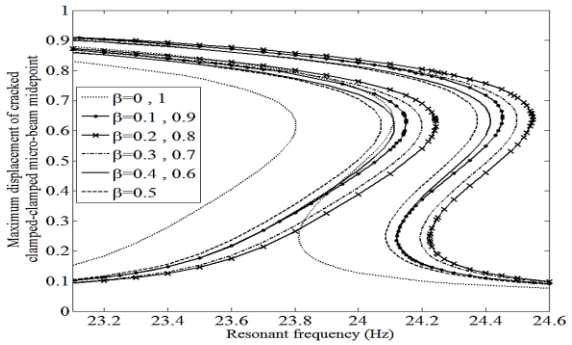

Fig.15
Frequency-response curves of midpoint of cracked clamped-clamped micro-beam for a fixed relative crack depth $n = 0.5$ and different crack locations at the onset of the pull-in instability: $V_{DC} = 2\ \mathrm{V}, V_{AC} = 0.1\mathrm{V}$.

Similarly, the frequency response of the midpoint of cracked clamped-clamped micro-beam under $V_{AC} = 0.1\mathrm{V}$ for a fixed relative crack location $\beta = 0.5$ and different crack depths is shown in Fig. 16. Fig. 16 shows that increasing the depth of crack decreases resonance frequency and increases rate of the changing of resonance frequency. Moreover, by increasing the depth of the crack, the cyclic-fold bifurcation appears at lower frequency and instability occurs faster.

To show the effect of the fringing field, the frequency-response curves of free end of cracked cantilever micro-beam is extracted for a fixed relative crack location $\beta = 0.05$ and crack depths $n = 0.5$ at the onset of the pull-in instability: $V_{DC} = 5\ \mathrm{V}, V_{AC} = 0.1\mathrm{V}$ (see Fig. 17). In this figure the solid line is the frequency response of cracked micro-beam by applying the fringing filed force and the dashed line is the frequency response of cracked micro-beam without the fringing filed. As can see in this figure the fringing field has very low effect on the frequency response of the cracked micro-beam and it is negligible.

Similarly, the frequency-response curves of midpoint of cracked clamped-clamped micro-beam is shown in Fig. 18 for a fixed relative crack location $\beta = 0{,}1$ and crack depths $n = 0.5$ at the onset of the pull-in instability: $V_{DC} = 2\ \mathrm{V}, V_{AC} = 0.1\mathrm{V}$. In this figure the solid line is the frequency response of cracked micro-beam by applying the fringing filed and the dashed line is the frequency response of cracked micro-beam without the fringing filed. As can see in this figure both curves are very similar to gether.

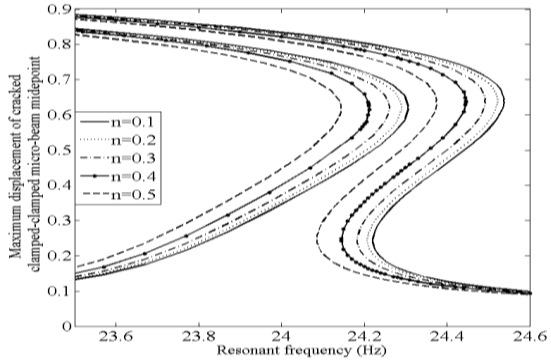

Fig.16
Frequency-response curves of midpoint of cracked clamped-clamped micro-beam for a fixed relative crack location $\beta = 0.5$ and different crack depths at the onset of the pull-in instability: $V_{DC} = 2\ \mathrm{V}, V_{AC} = 0.1\mathrm{V}$.

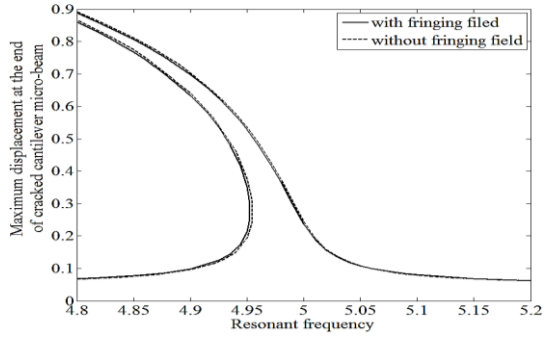

Fig.17
Frequency-response curves of free end of cracked cantilever micro-beam for a fixed relative crack location $\beta = 0.05$ and crack depths $n = 0.5$ at the onset of the pull-in instability: $V_{DC} = 5\ \mathrm{V}, V_{AC} = 0.1\mathrm{V}$.

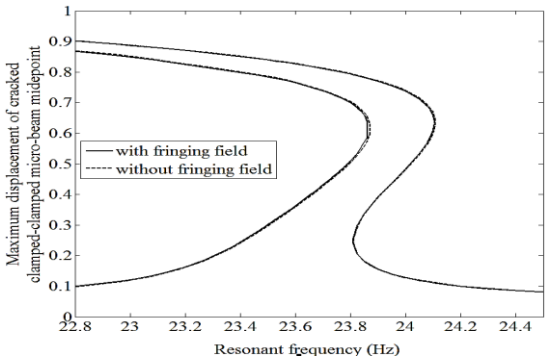

Fig.18
Frequency-response curves of midpoint of cracked clamped-clamped micro-beam for a fixed relative crack location $\beta = 0{,}1$ and crack depths $n = 0.5$ at the onset of the pull-in instability: $V_{DC} = 2\ \mathrm{V}, V_{AC} = 0.1\mathrm{V}$.

6 CONCLUSIONS

The electrostatically actuated MEMS devices are designed and produced to work in a special condition. Therefore the changes in the conditions or failure lead to malfunction and collapse of the micro-beam or the same pull-in phenomenon. Crack is one of the main faults that may be initiated and grown during the machining or under other factors. It was shown in this paper that the presence of the crack in the micro-beams leads to changes on the dynamic characteristics such as pull-in voltage and resonance frequency and resonance amplitude near the natural frequency. One can use these changes in sensors health monitoring applications. In this paper the dynamic behavior of cracked micro-electromechanical resonators was analyzed under AC and DC loading by applying residual axial force. The effect of the crack on the static and dynamic pull-in phenomenon was investigated. Since the ratio of the width of micro-beam *b* to capacitor gap width *d* is large, the effect of the fringing field force on the excitation force is less than 2 % for cantilever and 1 % for clamped-clamped cracked micro-beam and then it was neglected. The curves of the equilibria and the static pull-in voltage of micro-beam with cantilever and clamped-clamped boundary condition were extracted for different crack locations and crack depths. It follows from Figs. 2 to 5, the crack has slight influence on the static pull-in voltage and the changes of static pull-in voltage for crack location are more than the changes for crack depth.

Then curves of the frequency response of cracked cantilever and clamped-clamped micro-beam were extracted near natural frequency for different crack locations and depths. The dynamic behavior of cracked micro-beam is different from ordinary cracked beam, because of nonlinear effects. The dynamic behavior of clamped-clamped micro-beam according to parameter $\alpha_2 V_{DC}^2$ is hardening and the cantilever micro-beam is softening bellow the pull-in instability. As can be seen from the frequency response curves of cracked cantilever micro-beam bellow the pull-in instability, by approaching the crack to fixed end or increasing the crack depth, the resonance amplitude and softening phenomenon are increased and resonance frequency is reduced. Also, in cracked clamped-clamped micro-beam, the most reduction of resonance frequency and increasing in resonance amplitude occur at the fixed ends. By changing the location of the crack from the fixed end to relative location $\beta = 0.25,$ the resonance frequency increases and the resonance amplitude decreases. Then the resonance frequency decreases and the resonance amplitude increases by changing the location of the crack from the relative location $\beta = 0.25,$ to middle of the micro-beam. This procedure similarly repeats from $\beta = 1$ to middle of the micro-beam. In the cracked clamped-clamped micro-beam, by increasing the crack depth, the resonance amplitude increases and resonance frequency reduces. The researches of this paper show that the effect of crack on the dynamic response is more than static response and then the dynamic response is more suitable for crack identification. As shown in the curves of the frequency response of cracked cantilever micro-beam at the onset of pull-in instability condition, increasing the crack depth or approaching the crack to the fixed end causes the resonance frequency to decrease and the instability and pull-in phenomenon to occur at lower frequency. In the curves of frequency response of the cracked clamped-clamped micro-beam at the onset of pull-in instability condition, there are three cyclic-fold bifurcation. The behavior of the frequency response of cracked micro-beam is suddenly changed in these points and it may pull-in. The crack leads these points to appear at the lower frequency. Therefore, it causes early pull-in phenomenon or unwanted rathe change at the micro-beam behavior. Also, as shown in Figure 16, the effects of crack on the cyclic-fold bifurcation points are more than the other points and the curves are separated from each other near these points for different crack depths and crack locations.

REFERENCES

[1] Vardan V. M., Vinoy K. J., Jose K. A., 2003, *RF MEMS and their Applications*, Wiley, New York.

[2] Younis M. I., Nayfeh A. H., 2009, A study of the nonlinear response of a resonant micro-beam to an electric actuation, *Nonlinear Dynamic* **3**(1): 91-117.

[3] Rezazadeh G., Tahmasebi A., Ziaei-rad S., 2009, Nonlinear electrostatic behavior for two elastic parallel fixed-fixed and cantilever micro-beams, *Mechatronics* **19**: 840-846.

[4] Valilou S., Jalilpour M., 2012, Frequency response analysis of a capacitive micro-beam resonator considering residual and axial stresses and temperature changes effects, *Journal of Solid Mechanics* **4**(4): 416-425.

[5] Osterberg P. M., Senturia S. D., 1997, M-TEST: A test chip for MEMS material property measurement using electrostatically actuated test structures, *Micro-Electromechanical Systems* **6**(2): 107-118.

[6] Zhang Y., Zhao Y., 2006, Numerical and analytical study on the pull-in instability of micro-structure under electrostatic loading, *Sensor Actuator A* **127**: 366-380.

[7] Rezazadeh G., Tahmasebi A., Ziaei-rad S., 2009, Nonlinear electrostatic behavior for two elastic parallel fixed-fixed and cantilever micro-beams, *Mechatronics* **19**: 840-846.

[8] Mojahedi M., Moghimi zand M., Ahmadian M.T, 2010, Static pull-in analysis of electrostatically actuated microbeams using homotopy perturbation method, *Applied Mathematical Modeling* **34**: 1032-104.

[9] Wang Y.G., Lin W.H., Feng Z. J., Li X. M., 2012, Characterization of extensional multi-layer microbeams in pull-in phenomenon and vibrations, *Mechanical Sciences* **54**: 225-233.

[10] Mohammad T. F., Ouakad H. M., 2016, Static, eigenvalue problem and bifurcation analysis of MEMS arches actuated by electrostatic fringing-fields, *Microsystem Technologies* **22**: 193-206.

[11] Younis M.I., 2015, Analytical expressions for the electrostatically actuated curled beam problem, *Microsystem Technologies* **21**: 1709-1717.

[12] Mohammad-Alasti B., Rezazadeh G., Abbasgholipour M., 2012, Effect of temperature changes on dynamic pull-in phenomenon in a functionally graded capacitive micro-beam, *Journal of Solid Mechanics* **4**(3): 277-295.

[13] Nayfeh A.H., Younis M.I., Abdel-Rahman E.M., 2007, Dynamic pull-in phenomenon in MEMS resonators, *Nonlinear Dynamic* **48**: 153-163.

[14] Rezazadeh G., Fathalilou M., Sadeghi M., 2011, Pull-in voltage of electrostatically-actuated micro-beams in terms of lumped model pull-in voltage using novel design corrective coefficients, *Sensing and Imaging* **12**: 117-131.

[15] Sedighi H.M., Shirazi K.H., Changizian M., 2015, Effect of the amplitude of vibrations on the pull-in instability of doubled-sided actuated microswitch resonators, *Applied Mechanics and Technical Physics* **56**(2): 304-312.

[16] Muhlstein C., Brown S., 1997, Reliability and fatigue testing of MEMs, *Tribology Issues and Opportunities in MEMS* **1997**: 519-528.

[17] Motallebi A., Fathalilou M., Rezazadeh G., 2012, Effect of the open crack on the pull-in instability of an electrostatically actuated Micro-beam, *Acta Mechanica Solidica Sinica* **25**(6): 627-637.

[18] Zhou H., Zhang W. M., Peng Z. K., Meng G., 2015, Dynamic characteristics of electrostatically actuated micro-beams with slant crack, *Mathematical Problems in Engineering* **2015**: 1-13.

[19] Sourki R., Hoseini S.A.H., 2016, Free vibration analysis of size-dependent cracked microbeam based on the modified couple stress theory, *Applied Physics A* **122**: 1-11.

[20] Younis M.I., Abdel-Rahman E.M., Nayfeh A.H., 2002, Static and dynamic behavior of an electrically excited resonant microbeam, *Proceedings of the 43rd Conference on AIAA Structures, Structural Dynamics, and Materials*, Denver, Colorado.

[21] Abdel-Rahman E.M., Younis M.I., Nayfeh A.H. 2002, Characterization of the mechanical behavior of an electrically actuated micro-beam, *Micromechanical and Microengineering* **12**: 795-766.

[22] Lin H. P., Chang S. C., Wu J. D., 2002, Beam vibrations with an arbitrary number of cracks, *Sound and Vibration* **258**(5): 987-999.

[23] Younis M.I., 2010, *MEMS Linear and Nonlinear Statics and Dynamics*, Ph.D. thesis, State University of New York.